

Two Step Time Discretization of Willmore Flow

Nadine Olischläger and Martin Rumpf

Institut für Numerische Simulation,
Rheinische Friedrich-Wilhelms-Universität Bonn,
Nussallee 15, 53115 Bonn, Germany
{nadine.olischlaeger,martin.rumpf}@ins.uni-bonn.de,
WWW home page: <http://numod.ins.uni-bonn.de/>

Abstract. Based on a natural approach for the time discretization of gradient flows a new time discretization for discrete Willmore flow of polygonal curves and triangulated surfaces is proposed. The approach is variational and takes into account an approximation of the L^2 -distance between the surface at the current time step and the unknown surface at the new time step as well as a fully implicit approximation of the Willmore functional at the new time step. To evaluate the Willmore energy on the unknown surface of the next time step, we first ask for the solution of an inner, secondary variational problem describing a time step of mean curvature motion. The time discrete velocity deduced from the solution of the latter problem is regarded as an approximation of the mean curvature vector and enters the approximation of the actual Willmore functional. To solve the resulting nested variational problem in each time step numerically relaxation theory from PDE constraint optimization are taken into account. The approach is applied to polygonal curves and triangular surfaces and is independent of the co-dimension. Various numerical examples underline the stability of the new scheme, which enables time steps of the order of the spatial grid size.

1 Introduction

In this paper a new scheme for the time and space discretization of parametric Willmore flow is presented. Willmore flow is the L^2 gradient flow of surfaces for the Willmore energy, which measures the squared mean curvature on the surface. Let \mathcal{M} be a closed d -dimensional surface embedded in \mathbb{R}^m with $m \geq d + 1$ and denote by x the identity map on $\mathcal{M} = \mathcal{M}[x]$. Then the Willmore energy is defined as

$$w[x] := \frac{1}{2} \int_{\mathcal{M}} \mathbf{h}^2 \, da$$

where \mathbf{h} is the mean curvature on \mathcal{M} , i. e., \mathbf{h} is the sum of the principle curvatures on \mathcal{M} . Furthermore, the L^2 -metric $\int_{\mathcal{M}} v_1 v_2 \, da$ measures variations $x + v_i n$ of the surface \mathcal{M} in direction of the surface normal n . Given energy and metric the corresponding gradient flow – the Willmore flow – in the hypersurface case (cf.

Figure 1) ($m = d + 1$) is given by the following fourth order parabolic evolution problem

$$\partial_t x(t) = \Delta_{\mathcal{M}(t)} \mathbf{h}(t) n(t) + \mathbf{h}(t) (|S(t)|_2^2 - \frac{1}{2} \mathbf{h}(t)^2) n(t),$$

which defines for a given initial surface \mathcal{M}_0 a family of surfaces $\mathcal{M}(t)$ for $t \geq 0$ with $\mathcal{M}(0) = \mathcal{M}_0$ problem [29, 27, 18]. Here, $\Delta_{\mathcal{M}(t)}$ is the Laplace Beltrami operator on $\mathcal{M}(t)$, $S(t)$ denotes the shape operator on $\mathcal{M}(t)$, $n(t)$ the normal field on $\mathcal{M}(t)$, and $|\cdot|_2$ the Frobenius norm on the space of endomorphisms on the tangent bundle $\mathcal{TM}(t)$. The Willmore functional is used e.g. for the modeling of elastic surfaces [23, 22, 30, 8]. The analytic treatment of the Willmore flow has been considered by Polden [24, 25] and sharp results on long time existence and regularity were obtained by Kuwert and Schätzle [18, 20, 19]. Willmore flow for curves is called elastic flow of curves (cf. Figure 1) and has been considered by Dziuk, Kuwert and Schätzle in [16]. A level set formulation has been developed by [13]. We refer to Deckelnick and Dziuk [10] for the convergence analysis in the graph case and to Barrett, Garcke and Nürnberg [1], Bobenko and Schröder [5] and Dziuk [17] for alternative numerical methods for Willmore flow on triangular surfaces. In imaging fourth order problem are very popular in the context of image inpainting and surface restoration [4, 3, 9, 26]. Apart from fully explicit time discretizations these numerical approach are characterized by a semi-implicit time discretization, which requires the solution of a linear system of equations in each time step. One observes significant restrictions on the time step size. Effectively, one usually has to enforce time steps $\tau = O(h^2)$, where h was the spatial grid size.

This shortcoming motivated the development of a new concept for the time discretization of Willmore flow picking up the variational time discretization of general gradient flows. Given an energy $e[\cdot]$ on a manifold the gradient flow $\dot{x} = -\text{grad}_g e[x]$ with initial data x^0 one defines a sequence of time discrete solutions $(x^k)_{k=0, \dots}$, where $x_k \approx x(k\tau)$ for the time step size τ via a variational problem, to be solved in each time step, i.e.

$$x^{k+1} = \arg \min_x \text{dist}(x, x^k)^2 + 2\tau e[x]$$

where $\text{dist}(x, x^k) = \inf_{\gamma \in \Gamma} \int_0^1 \sqrt{g_{\gamma(s)}(\dot{\gamma}(s), \dot{\gamma}(s))} ds$ is the shortest path length on the manifold, given the metric $g(\cdot, \cdot)$. Here Γ denotes the set of smooth curves γ with $\gamma(0) = x^k$ and $\gamma(1) = x$. As an immediate consequence, one obtains the energy estimate $e[x^{k+1}] + \frac{1}{2\tau} \text{dist}(x^{k+1}, x^k)^2 \leq 0 + e[x^k]$. For geometric problems, this approach has already been considered by Luckhaus and Sturzenhecker [21] in case of mean curvature motion, which is the L^2 gradient flow of the surface area. They proposed a corresponding fully implicit time discretization based on a variational problem in BV to be solved in each time step. In fact, in each time step the symmetric distance between two consecutive shapes corresponding to the current and the next time step is balanced by the time step τ times the perimeter of the shape at the next time step. Chambolle [7] investigated a reformulation of this approach in terms of a level set method. A related method for

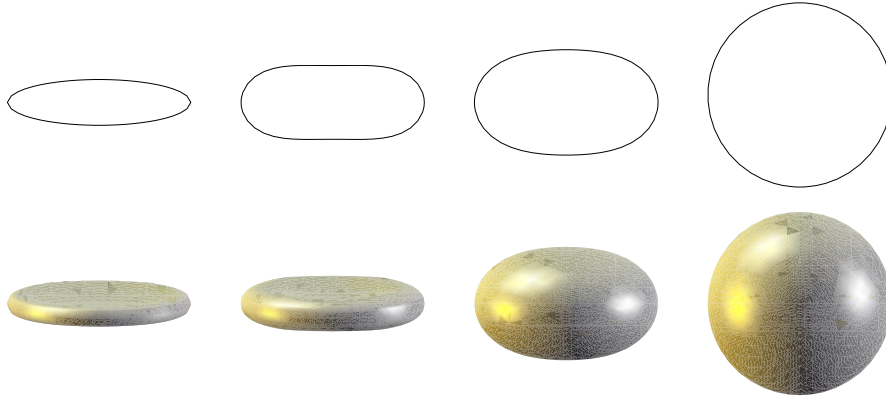


Fig. 1. Different time steps of the Willmore flow of an original ellipsoid curve with 100 vertices is shown (top row). The time step size was chosen of the order of the spatial grid size $h = \tau = 0.0632847$. Willmore flow of a deformed sphere towards a round sphere is depicted in the bottom row. We show the surface at times $t = 0$, $t = \tau$, $t = 50\tau$, and $t = 150\tau$, where $\tau = h = 0.02325548045$.

anisotropic mean curvature motion is discussed in [2, 6].

In case of Willmore flow, we will proceed as follows. We aim at balancing the squared distance of the unknown surface at time $t_{k+1} = t_k + \tau$ from the current surface at time t_k and a suitable approximation of the Willmore energy at time t_{k+1} scaled by twice the time step size. Solving a fully implicit time discrete problem for mean curvature motion for the unknown surface at time t_{k+1} , we can regard the corresponding difference quotient in time as a time discrete, fully implicit approximation of the mean curvature vector. Based on this mean curvature vector, the Willmore functional can be approximated. Thus, we are lead to a nested minimization problem in each time step. In the inner problem on the new time step an implicit mean curvature vector is identified. Then, the outer problem is the actual implicit, variational formulation of Willmore flow. Indeed, the resulting two step time discretization experimentally turns out to be unconditionally stable and effectively allows for time steps of the order of the spatial grid size.

The paper is organized as follows. In Section 2 we derive the time discrete scheme for Willmore flow, still continuous in space. Based on piecewise affine finite elements on simplicial surfaces we derive a fully discrete numerical approach in Section 3. In Section 4 the duality technique from PDE constraint optimization is revisited to derive a minimization algorithm for the optimization problem. Finally, in Section 5 various examples for the Willmore of curves and surfaces are investigated.

2 Derivation of the two step time discretization

Before we consider the actual time discretization of Willmore flow, let us briefly review the time discretization of mean curvature motion. Following the above abstract approach the variational time discretization of mean curvature motion for a given surface $\mathcal{M} = \mathcal{M}[x]$ defines the mapping $y = y[x]$ of the next time step surface $\mathcal{M}[y]$ as the minimizer of the functional $\text{dist}(\mathcal{M}[y], \mathcal{M}[x])^2 + 2\tilde{\tau} \int_{\mathcal{M}[y]} da$, where $\tilde{\tau}$ is the considered time step, $\text{dist}(\cdot, \cdot)$ is the L^2 distance between surfaces, and $\int_{\mathcal{M}[y]} da$ the surface area of $\mathcal{M}[y]$ as the underlying energy. Now, for y close to x , we can consider a first order expansion in time and obtain the following variational problem: Given a surface $\mathcal{M}[x]$ parameterized by a mapping x we ask for a mapping $y = y[x]$, which minimizes the functional

$$e[x, y] = \int_{\mathcal{M}[x]} (y - x)^2 + \tilde{\tau} |\nabla_{\mathcal{M}[x]} y|^2 da$$

for given x . In what follows the time step size $\tilde{\tau}$ is chosen independent of the time step size for the actual time discrete Willmore flow. In our later spatially discrete model we consider a $\tilde{\tau}$ equal to the square of the spatial grid size. The resulting weak form of the corresponding Euler-Lagrange equations is

$$0 = \int_{\mathcal{M}[x]} (y - x) \cdot \theta + \tilde{\tau} \nabla_{\mathcal{M}[x]} y : \nabla_{\mathcal{M}[x]} \theta da$$

for some test function θ , where $A : B = \text{tr}(A^T B)$. This equation coincides with the nowadays classical scheme for a single semi-implicit time step of mean curvature motion already proposed by Dziuk [15].

Now, we deduce from the time continuous evolution equation $\partial_t x = \mathbf{h}n$ that the difference quotient $\frac{y[x]-x}{\tilde{\tau}}$ can be considered as a regularized approximation of the mean curvature vector $\mathbf{h}n$ on $\mathcal{M}[x]$. Thus, the functional $\frac{1}{2} \int_{\mathcal{M}[x]} \frac{(y[x]-x)^2}{\tilde{\tau}^2} da$ approximates the Willmore functional on $\mathcal{M}[x]$.

This enables us to define a time discretization of Willmore flow, which does not require the explicit evaluation of the mean curvature on the unknown surface of the next time step. Indeed, in the abstract variational problem

$$\text{dist}(\mathcal{M}[x], \mathcal{M}[x^k])^2 + \tau \int_{\mathcal{M}[x]} \mathbf{h}^2 da \rightarrow \min$$

we consider the same linearization of the L^2 distance as for mean curvature motion and use the above approximation of the Willmore energy. Finally, we obtain the following scheme:

Given an initial surface $\mathcal{M}[x^0]$ we define a sequence of surface $\mathcal{M}[x^k]$ with $k = 1, \dots$, where x^{k+1} minimizes the functional

$$w[x^k, x, y[x]] = \int_{\mathcal{M}[x^k]} (x - x^k)^2 da + \frac{\tau}{\tilde{\tau}^2} \int_{\mathcal{M}[x]} (y[x] - x)^2 da$$

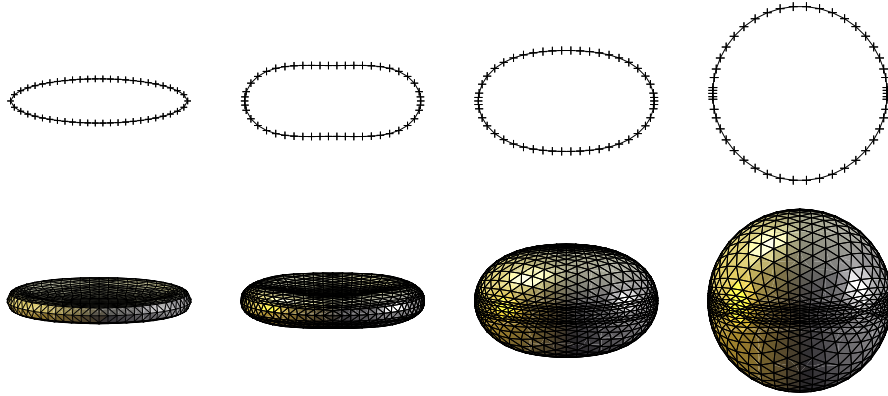


Fig. 2. The grids of the evolution under Willmore flow of the initial ellipsoid curve and deformed sphere of Figure 1 are shown at the same times. We did not reparametrize the curve since our scheme does not suffer from undesired tangential motions.

for given x_k . Hence, x^k is assumed to approximate $x(t_k)$ with $t_k = k\tau$ for the given time step τ .

Thus, in each time step we have to solve the nested variational problem

$$\begin{aligned} x^{k+1} &= \arg \min_x w[x^k, x, y[x]] \quad \text{with} \\ y[x] &= \arg \min_y e[x, y]. \end{aligned} \quad (1)$$

The inner problem is quadratic, hence the Euler–Lagrange equation is a linear elliptic PDE and we end up with a PDE constrained optimization problem for each time step.

To be more explicit, let us examine circles in the plane. Under Willmore flow circles expand according the ODE $\dot{R}(t) = \frac{1}{2}R(t)^{-3}$ for the radius. In comparison to this the radius R^{k+1} in the above time discrete scheme turns out to be a solution of the nonlinear equation $\frac{R-R_k}{\tau} = \frac{1}{2} \frac{R^4 - 3R^2\tau}{(R^2 + \tau)^3 R_k}$, which is an implicit first order scheme for the above ODE (cf. Figure 3).

3 Finite element space discretization

In this section we introduce a suitable space discretization based on piecewise affine finite elements. Here, we follow the guideline for finite elements on surfaces introduced by [14]. Thus, we consider simplicial meshes $\mathcal{M}[X]$ - polygonal curves for $d = 1$ and triangular surfaces for $d = 2$ - as approximations of the d dimensional surfaces $\mathcal{M}[x]$. Here, X is the identity on the simplicial mesh $\mathcal{M}[X]$ which is described by a vector \bar{X} of vertex positions of the mesh. To clarify the notation we will always denote discrete quantities with upper case letters to distinguish them from the corresponding continuous quantities in lower case letters. Furthermore, a bar on top of a discrete function indicates the corresponding nodal

vector, i.e. $\bar{X} = (\bar{X}_i)_{i \in I}$, where $\bar{X}_i = (X_i^1, \dots, X_i^m)$ is the coordinate vector of the i th vertex of the mesh and I denotes the index set of vertices.

Hence, given some initial surface $\mathcal{M}[X^0]$ we seek a sequence of discrete surfaces $(\mathcal{M}[X^k])_{k=1, \dots}$ of discrete surfaces. Locally, using also local indices each element T of a polygonal curve is a line segment with nodes X_1 and X_2 and elements T of a triangulation are planar triangles with vertices X_0, X_1 , and X_2 and face vectors $F_0 = X_2 - X_1$, $F_1 = X_0 - X_2$, and $F_2 = X_1 - X_0$. Given a simplicial surface $\mathcal{M}[X]$ we denote by

$$\mathcal{V}(\mathcal{M}[X]) := \{U \in C^0(\mathcal{M}[X]) \mid \Phi|_T \in \mathcal{P}_1 \forall T \in \mathcal{M}[X]\}.$$

the corresponding piecewise affine Finite Element space consisting of those functions being affine on each element T of $\mathcal{M}[X]$. With a slight misuse of notation the mapping X itself is considered as an element in $\mathcal{V}(\mathcal{M}[X])^m$. Let $\{\Phi_i\}_{i \in I}$ be the nodal basis of $\mathcal{V}(\mathcal{M}[X])$. Thus, for $U \in \mathcal{V}(\mathcal{M}[X])$ we obtain $U = \sum_{i \in I} U(X_i) \Phi_i$ and $\bar{U} = (U(X_i))_{i \in I}$, in particular in accordance to our above definition we recover $\bar{X} = (X_i)_{i \in I}$.

Next, let us introduce the mass matrix $M[X]$ and the stiffness matrix $L[X]$ on the discrete surface $\mathcal{M}[X]$, whose entries are given by

$$M_{ij}[X] = \int_{\mathcal{M}[X]} \Phi_i \Phi_j \, da, \quad L_{ij}[X] = \int_{\mathcal{M}[X]} \nabla_{\mathcal{M}[X]} \Phi_i \cdot \nabla_{\mathcal{M}[X]} \Phi_j \, da.$$

To apply mass and stiffness matrices to discrete maps from $\mathcal{M}[X]$ to \mathbb{R}^m , we need corresponding block matrices $\mathbf{M}[X]$ and $\mathbf{L}[X]$ in $\mathbb{R}^{m \# I \times m \# I}$:

$$\mathbf{M}[X] = \begin{pmatrix} M[X] & & \\ & M[X] & \\ & & M[X] \end{pmatrix}, \quad \mathbf{L}[X] = \begin{pmatrix} L[X] & & \\ & L[X] & \\ & & L[X] \end{pmatrix}.$$

Both, mass and stiffness matrix M and L can be assembled from corresponding local mass and stiffness matrices $m(T)$ and $l(T)$ for all simplices T on $\mathcal{M}[X]$.

Now, we have all the ingredients at hand to derive the fully discrete two step time discretization of Willmore flow (cf. Figure 2), which is can be regarded as discrete counterpart of (1). Given a discrete surface $\mathcal{M}(X^k)$ in time step k we define $X^{k+1} \in \mathcal{V}(\mathcal{M}[X^k])^m$ as the minimizer of the following spatially discrete, nested variational problem

$$\begin{aligned} X^{k+1} &= \arg \min_{X \in \mathcal{V}(\mathcal{M}[X^k])^m} W[X^k, X, Y[X]] \quad \text{with} \quad (2) \\ Y[X] &= \arg \min_{Y \in \mathcal{V}(\mathcal{M}[X])^m} E[X, Y], \end{aligned}$$

where

$$\begin{aligned}
E[X, Y] &:= \int_{\mathcal{M}[X]} (Y - X)^2 + \tilde{\tau} |\nabla_{\mathcal{M}[X]} Y|^2 \, da \\
&= \mathbf{M}[X](\bar{Y} - \bar{X}) \cdot (\bar{Y} - \bar{X}) + \tilde{\tau} \mathbf{L}[X] \bar{Y} \cdot \bar{Y}, \\
W[X^k, X, Y] &:= \int_{\mathcal{M}[X^k]} (X - X^k)^2 \, da + \frac{\tau}{\tilde{\tau}^2} \int_{\mathcal{M}[X]} (Y - X)^2 \, da \\
&= \mathbf{M}[X^k](\bar{X} - \bar{X}^k) \cdot (\bar{X} - \bar{X}^k) + \frac{\tau}{\tilde{\tau}^2} \mathbf{M}[X](\bar{Y} - \bar{X}) \cdot (\bar{Y} - \bar{X})
\end{aligned}$$

are the straightforward spatially discrete counterpart of the functionals $e[x, y]$ and $w[x^k, x, y]$, respectively. In analogy to the continuous case for given X the nodal vector $\bar{Y}[X]$ solves the a linear system of equation

$$(\mathbf{M}[X] + \tilde{\tau} \mathbf{L}[X]) \bar{Y}[X] = \mathbf{M}[X] \bar{X}. \quad (3)$$

For the sake of completeness let us finally give explicit formulas for the entries of the mass and stiffness matrices. Later in Section 4 we will have to compute variations of these entries as well.

Polygonal curve. In the case of curves we consider a lumped mass matrix (cf. [28]) and obtain directly for the global matrices

$$M[X] = \text{diag} \left(\frac{1}{2}(Q_i + Q_{i+1}) \right), \quad L[X] = \text{tridiag} \left(-\frac{1}{Q_i}, \frac{1}{Q_i} + \frac{1}{Q_{i+1}}, -\frac{1}{Q_{i+1}} \right)$$

where $Q_i = |X_i - X_{i-1}|$ is the length of the j th line segment and $\text{diag}()$ and $\text{tridiag}()$ denote diagonal or tridiagonal matrices with the corresponding entries in each row. Here, we assume a cyclic indexing, i.e. we identify the indices $i = 1$ and $i = \sharp I + 1$ for closed curves with $X_0 = X_{\sharp I}$.

Triangular surfaces. Due to the greater variability of triangular surfaces compared to polygonal curves, let us consider the local matrices on triangles separately. Denoting the local basis function on a triangle T by Φ_0, Φ_1, Φ_3 , where $\Phi_i(X_j) = \delta_{ij}$ (with δ_{ij} being the usual Kronecker symbol) we verify by a simple straightforward computation (cf. [12]) that

$$m(T) = \left(\int_T \Phi_i \Phi_j \, da \right)_{i,j=0,1,2} = \frac{|T|}{12} \begin{pmatrix} 2 & 1 & 1 \\ 1 & 2 & 1 \\ 1 & 1 & 2 \end{pmatrix},$$

with $|T| = \frac{1}{2} |F_2 \wedge F_1|$ being the area of the triangle T , and

$$l(T)_{ij} = \int_T \nabla_T \Phi_i \cdot \nabla_T \Phi_j \, da = \frac{F_i \cdot F_j}{4|T|},$$

where ∇_T the gradient on planar T .

4 Numerical solution of the optimization problem

In this section, we discuss how to numerically solve in each time step the non-linear optimization problem (2). Here, we will confine to a gradient descent approach and take into account a suitable duality technique to effectively compute the gradient of the energy functional $\hat{W}[X] = W[X^k, X, Y[X]]$ given the fact that the argument $Y[X]$ is a solution of the inner minimization problem and as such solves the linear system of equations (3). Indeed, we obtain for the variation of \hat{W} in a direction $\Theta \in \mathcal{V}(\mathcal{M}[X^k])^m$

$$\partial_X \hat{W}[X](\Theta) = \partial_X W[X^k, X, Y[X]](\Theta) + \partial_Y W[X^k, X, Y[X]] (\partial_X Y[X](\Theta)).$$

A direct computation of $\partial_X Y[X](\Theta)$ would require the solution of the inner minimization problem and thus specifically a linear system (cf. (3)) would have to be solved for every test function Θ . This can be avoided applying the following duality argument:

From the optimality of $Y[X]$ in the inner problem, we deduce the equation $0 = \partial_Y E[Y[X], X](\Psi)$ for any test function $\Psi \in \mathcal{V}(\mathcal{M}[X])^m$. Now, differentiating with respect to X we obtain

$$\begin{aligned} 0 &= \partial_X (\partial_Y E[Y[X], X](\Psi)) (\Theta) \\ &= \partial_X \partial_Y E[Y, X](\Psi, \Theta) + \partial_Y^2 E[Y[X], X](\Psi, \partial_X Y[X](\Theta)) \end{aligned}$$

for any test function Ψ . Let us now define $P \in \mathcal{V}(\mathcal{M}[X^k])^m$ as the solution of the dual problem

$$\partial_Y^2 E[Y[X], X](P, \Psi) = \partial_Y W[X^k, X, Y[X]](\Psi). \quad (4)$$

for all test functions $\Psi \in \mathcal{V}(\mathcal{M}[X^k])^m$. Now, choosing $\Psi = \partial_X Y[X](\Theta)$ one obtains

$$(\partial_Y W)[X^k, X, Y[X]] (\partial_X Y[X](\Theta)) = -\partial_X \partial_Y E[Y, X](P, \Theta).$$

Thus, we can finally rewrite the variation of \hat{W} with respect to X in a direction Θ as

$$\partial_X \hat{W}[X](\Theta) = \partial_X W[X^k, X, Y[X]](\Theta) - \partial_X \partial_Y E[Y, X](P, \Theta). \quad (5)$$

The solution P of the dual problem (4) requires to solve

$$\int_{\mathcal{M}[X]} P \cdot \Psi + \tilde{\tau} \nabla_{\mathcal{M}[X]} P : \nabla_{\mathcal{M}[X]} \Psi \, da = \int_{\mathcal{M}[X]} \frac{\tau}{\tilde{\tau}^2} (Y - X) \cdot \Psi \, da$$

for all test functions Ψ . In matrix vector notation, this can be written as the linear system of equations

$$(\mathbf{M}[X] + \tilde{\tau} \mathbf{L}[X]) \bar{P} = \frac{\tau}{\tilde{\tau}^2} \mathbf{M}[X] (\bar{Y} - \bar{X}).$$

The terms on the right hand side of (5) are to be evaluated as follows

$$\begin{aligned}
(\partial_X W)[X^k, X, Y](\Theta) &= 2 \mathbf{M}[X^k](\bar{X} - \bar{X}^k) \cdot \bar{\Theta} + 2 \frac{\tau}{\bar{\tau}^2} \mathbf{M}[X](\bar{X} - \bar{Y}) \cdot \bar{\Theta} \\
&\quad + \frac{\tau}{\bar{\tau}^2} (\partial_X \mathbf{M}[X](\Theta))(\bar{Y} - \bar{X}) \cdot (\bar{Y} - \bar{X}), \\
\partial_X \partial_Y E[Y, X](P, \Theta) &= \partial_X (2 \mathbf{M}[X](\bar{Y} - \bar{X}) \cdot \bar{P} + 2\bar{\tau} \mathbf{L}[X] \bar{Y} \cdot \bar{P}) (\Theta) \\
&= 2(\partial_X \mathbf{M}[X](\Theta))(\bar{Y} - \bar{X}) \cdot \bar{P} - 2 \mathbf{M}[X] \bar{\Theta} \cdot \bar{P} \\
&\quad + 2\bar{\tau} (\partial_X \mathbf{L}[X](\Theta)) \bar{Y} \cdot \bar{P}.
\end{aligned}$$

It remains to compute the variation of the mass and stiffness matrix with respect to a variation θ of the simplicial grid,

$$\begin{aligned}
\partial_X \mathbf{M}[X](\Theta) &= \begin{pmatrix} \partial_X M[X](\Theta) & & \\ & \partial_X M[X](\Theta) & \\ & & \partial_X M[X](\Theta) \end{pmatrix}, \\
\partial_X \mathbf{L}[X](\Theta) &= \begin{pmatrix} \partial_X L[X](\Theta) & & \\ & \partial_X L[X](\Theta) & \\ & & \partial_X L[X](\Theta) \end{pmatrix},
\end{aligned}$$

where $\partial_X M[X](\Theta) = \frac{d}{d\epsilon} M[X + \epsilon \Theta]|_{\epsilon=0}$ and $\partial_X L[X](\Theta) = \frac{d}{d\epsilon} L[X + \epsilon \Theta]|_{\epsilon=0}$. Finally, we can compute the descent direction in $\mathbb{R}^{m \# I}$ of the energy \hat{W} at a given simplicial mesh $\mathcal{M}[X]$ described by the nodal vector \bar{X} and obtain

$$\overline{\text{grad}_X \hat{W}[X]} = \left(\partial_X \hat{W}[X](\Phi_r e_s) \right)_{r \in I, s=1, \dots, m},$$

where e_s denotes the s th coordinate direction in \mathbb{R}^m .

In the concrete numerical algorithm we now perform a gradient descent method with the Amijo step size control starting from the initial position given by the previous time step.

Polygonal curve. We obtain for the derivatives of the mass matrix (using again the usual Kroneckersymbol δ_{ir}) with respect to a variation of node r in direction s

$$\partial_X M[X](\Phi_r e_s) = \text{diag} \left(\frac{(X_{i-1}^s - X_i^s)(\delta_{(i-1)r} - \delta_{ir})}{2Q_i} + \frac{(X_i^s - X_{i+1}^s)(\delta_{ir} - \delta_{(i+1)r})}{2Q_{i+1}} \right),$$

where as above $Q_i = |X_i - X_{i-1}|$. Furthermore, we get for the derivatives for the stiffness matrix in the same direction

$$\partial_X L[X](\Phi_r e_s) = \text{tridiag}(\partial_X L_{i-1}, \partial_X L_i, \partial_X L_{i+1}),$$

where

$$\begin{aligned}\partial_X L_{i-1} &:= \frac{(X_{i-1}^s - X_i^s)(\delta_{(i-1)r} - \delta_{ir})}{Q_i^3}, \\ \partial_X L_i &:= -\frac{(X_{i-1}^s - X_i^s)(\delta_{(i-1)r} - \delta_{ir})}{Q_i^3} - \frac{(X_i^s - X_{i+1}^s)(\delta_{ir} - \delta_{(i+1)r})}{Q_{i+1}^3}, \\ \partial_X L_{i+1} &:= \frac{(X_i^s - X_{i+1}^s)(\delta_{ir} - \delta_{(i+1)r})}{Q_{i+1}^3}.\end{aligned}$$

Triangular surfaces. The first variation of $|T|$ with respect to a variation of node r in direction s is given by

$$\partial_X |T|(\Phi_r e_s) = \frac{1}{2} \frac{F_1 \wedge F_2}{|F_1 \wedge F_2|} D_s^{90} P_s F_r,$$

where P_s is a projection onto the plane spanned by the vectors e_{s-1} and e_{s+1} and D_s^{90} a counter-clockwise rotation of 90 degree in this plane. It is suitable to assume vertex indices to be in $\{0, 1, 2\}$ and take them modulo 2 if this is not the case. Now, we obtain for the derivative of the local mass matrix with respect to a variation of node r in direction s

$$\partial_X m(T)(\Phi_r e_s) = \frac{\partial_X |T|(\Phi_r e_s)}{12} \begin{pmatrix} 2 & 1 & 1 \\ 1 & 2 & 1 \\ 1 & 1 & 2 \end{pmatrix}.$$

The corresponding derivative of the local stiffness matrix is given by

$$\begin{aligned}\partial_X l(T)_{ij}(\Phi_r e_s) &= \frac{1}{4|T|} ((\delta_{r(i-1)} - \delta_{r(i+1)})F_j^s + (\delta_{r(j-1)} - \delta_{r(j+1)})F_i^s) \\ &\quad - \frac{\partial_X |T|(\Phi_r e_s)}{4|T|^2} F_i \cdot F_j.\end{aligned}$$

5 Numerical results

We have applied the developed numerical algorithm to the evolution of curves in \mathbb{R}^2 and \mathbb{R}^3 and of two dimensional surfaces in \mathbb{R}^3 . Here, we present first results which in particular demonstrate the robustness of the proposed method. In fact, the applications underline that time steps up to the order the spatial grid size h are feasible.

Willmore flow for curves. At first we have studied the evolution of circles in \mathbb{R}^2 . Figure 3 shows that the numerical solution will approximate the known exact solution of expanding circles. In the next computations we consider a slight generalization of the above Willmore flow model. In fact, we add $\lambda a[x]$ to the Willmore energy, where λ is a fixed constant and $a[x]$ denotes the length of the

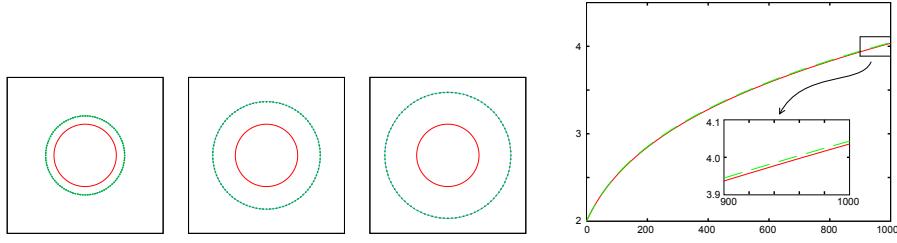


Fig. 3. A circle of radius $R_0 = 2$ expands in two dimension due to its propagation via Willmore flow (left). The exact solution (grey dashed line) and the corresponding discrete solution computed by the two step time discretization for 200 polygon vertices and a time step size which equals the grid size (green crosses) are plotted for different times $t = 100h, 500h, 1000h$. The radius of the growing circle under Willmore flow is plotted for the known continuous solution (green) and the discrete solution (red). (right)

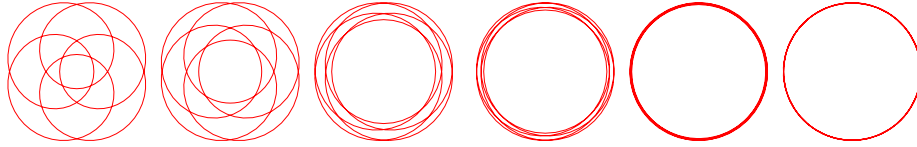


Fig. 4. The evolution of a planar hypocycloid towards a fivefold covering of a circle is shown at times $t = 0.0, t = 685.7, t = 2987.4, t = 4850.1, t = 7965.8, t = 10630.6$. The curves are graphically rescaled to have similar size. Here the computational parameters were $\lambda = 0.025, N = 200$ and $\tau = h = 0.5493$.

curve. Here, λ can be regarded as a Lagrangian multiplier with respect to a length constraint. Hence, for proper choices of λ the generalized model avoids expansion.

If X represents a discrete closed curve as above, we obtain for the discrete length functional $A[X] = \sum_{i \in I} Q_i$. Furthermore, its gradient vector in $\mathbb{R}^{m \cdot I}$ is given by $\overline{\text{grad}}_X A[\overline{X}] = L[X]\overline{X}$.

As a first example for the resulting flow we consider the evolution of an ellipse towards a circle under the elastic flow (cf. the first rows in Figure 1 and 2).

The initial parametrization is given as

$$x_0(t) = (\sin(t), 4 \cos(t), 0) \text{ for } t \in [0, 2\pi].$$

The computational parameters are $h = 0.0632847, \tau = h$ and $\lambda = 0.025$. One observes that the ellipse evolves to a circle and the polygonal vertices stay well-distributed on the evolving curve. In the next application we pick up an example already discussed by Dziuk and Deckelnick in [11], where a hypocycloid is considered as initial data. Here, the parametrization of the initial curve is given

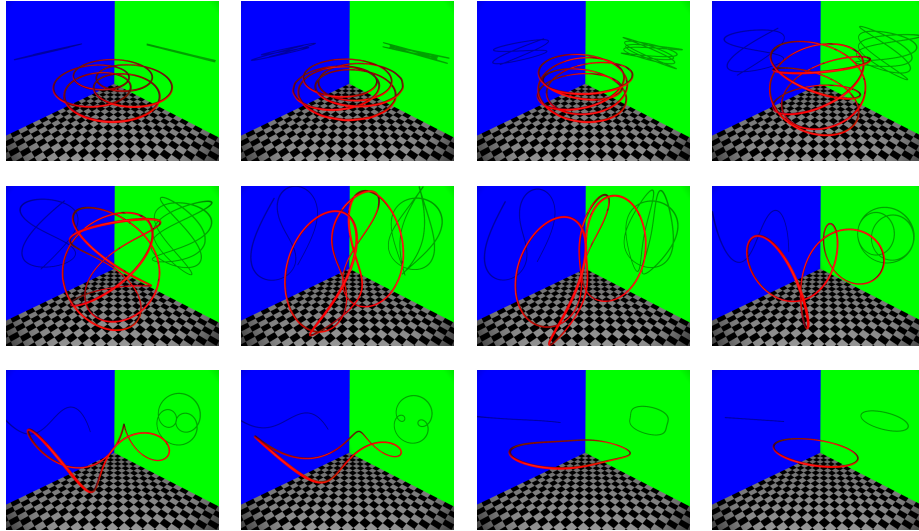


Fig. 5. Evolution of a vertically perturbed hypocycloid towards a circle under Willmore flow is shown at times $t = 0.0$, $t = 1348.9$, $t = 4467.1$, $t = 5511.4$, $t = 6555.7$, $t = 7406.6$, $t = 8257.2$, $t = 9108.4$, $t = 9297.0$, $t = 9361.3$, $t = 9426.8$, $t = 9489.1$. The computational data were $\delta = 0.1$, $\lambda = 0.025$, $N = 200$ and $\tau = h = 0.5$.

by

$$X_0(t) = \left(-\frac{5}{2} \cos(t) + 4 \cos(5t), -\frac{5}{2} \sin(t) + 4 \sin(5t), \delta \sin(3t) \right)$$

with $\delta = 0$. In \mathbb{R}^2 the initial curve evolves to a fivefold covering of a circle (cf. Figure 4) since multiple coverings of a circle are stable stationary solutions in the codimension one case [25]. This is not true for higher codimension with $m \geq 3$. If we start with an initial curve slightly perturbed in vertical direction, we have chosen $\delta = 0.1$, the curve begins to unfold and evolves to a single circle (cf. Figure 5).

Willmore flow for surfaces. Spheres are minima of the Willmore functional with energy 8π . In our first example for two dimensional surfaces in \mathbb{R}^3 we show the evolution of a cubical surface into a round sphere (cf. Figure 6). In Figure 7 we depict the evolution of a coarse polygonal approximation of a torus towards the Clifford torus $\mathcal{M} = \{x \in \mathbb{R}^3 | (1 - \sqrt{x_1^2 + x_2^2})^2 + x_3^2 = \frac{1}{2}\}$. Finally, in Figure 8 we compare the discrete evolution at a fixed time for different choices of the time step τ used in the computation.

Acknowledgement

Nadine Olischläger has been supported by the DFG collaborative research center SFB 611 at Bonn University and the Hausdorff Center for Mathematics.

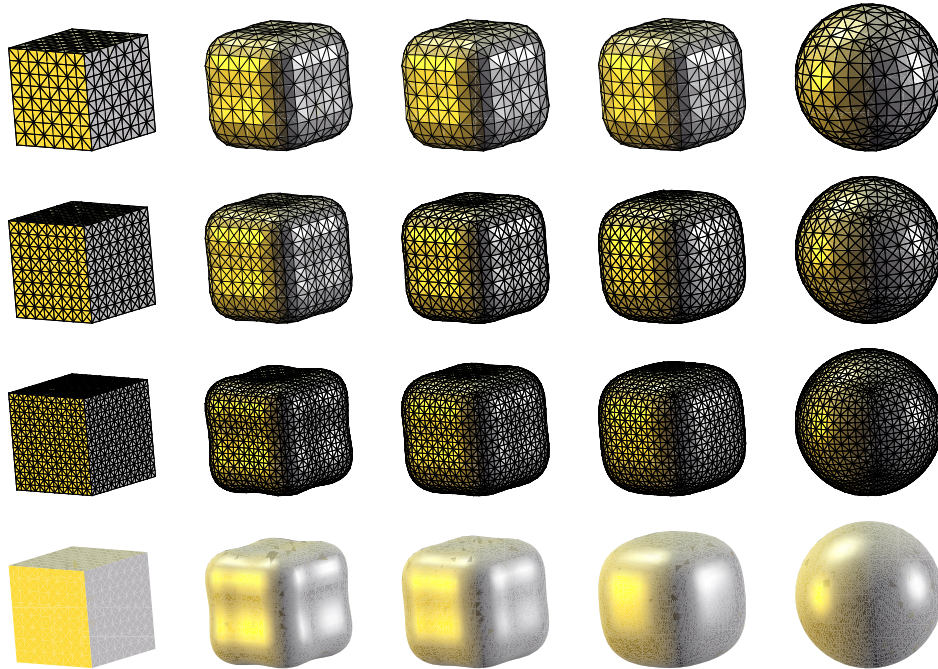


Fig. 6. Willmore flow for an initial cubical surface with 768 (1st row), 1536 elements (2nd row), and 3072 elements (4th, 5th rows) are shown at times $t = 0.0$, $t = 0.0366$, $t = 0.0732$, $t = 0.1464$, and $t = 0.366$, where $h = 0.07322$, $h = 0.0517766$, and $h = 0.0366$, respectively.

Furthermore, the authors are grateful to Orestis Vantzios for helping with the rendering in Figure 5.

References

1. J. W. Barrett, H. Garcke, and R. Nürnberg. A parametric finite element method for fourth order geometric evolution equations. *J. Comp. Phys.*, 222:441–467, 2007.
2. G. Bellettini, V. Caselles, A. Chambolle, and M. Novaga. Crystalline mean curvature flow of convex sets. Technical Report 7641, UMR CNRS, October 2004.
3. M. Bertalmio, A.L. Bertozzi, and G. Sapiro. Navier-stokes, fluid dynamics, and image and video inpainting. In *IEEE Proceedings of the International Conference on Computer Vision and Pattern Recognition*, volume 1, pages 355–362, 2001.
4. M. Bertalmio, G. Sapiro, V. Caselles, and C. Ballester. Image inpainting. In *Proc. of SIGGRAPH 2000*, pages 417–424, New Orleans, USA, July 2000.
5. A. Bobenko and P. Schröder. Discrete Willmore flow. In *SIGGRAPH (Courses)*. ACM Press, 2005.
6. A. Chambolle and M. Novaga. Convergence of an algorithm for anisotropic mean curvature motion. *SIAM J. Math. Anal.*, 37:1978–1987, 2006.
7. Antonin Chambolle. An algorithm for mean curvature motion. *Interfaces and free Boundaries*, 6:195–218, 2004.

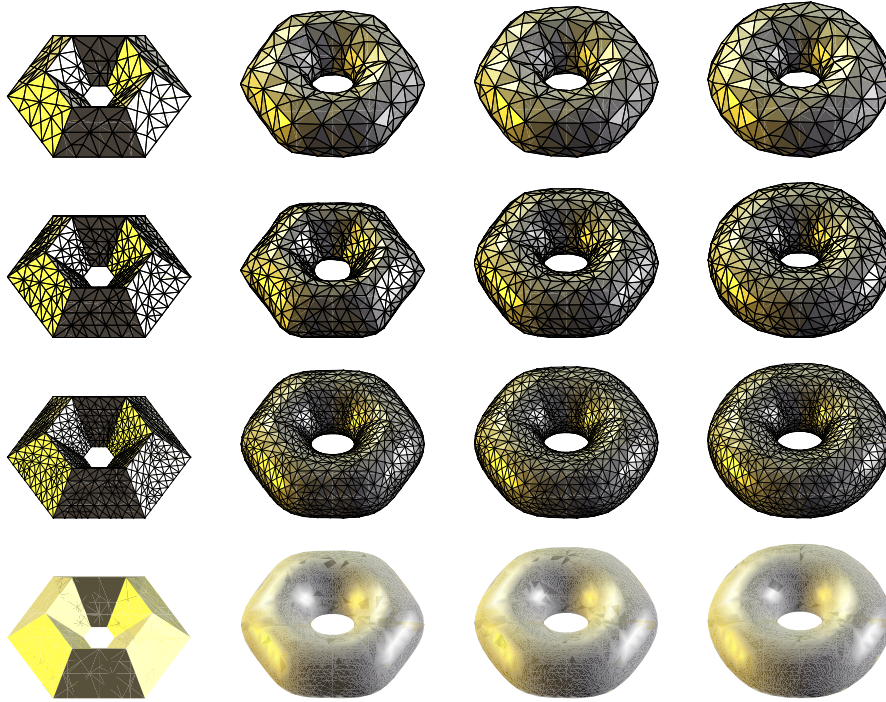


Fig. 7. Different time steps of Willmore flow towards a sphere for an initial macro torus with 522 (first row), 1224 (second row), and 2736 elements (third and fourth row). We render the surfaces at times $t = 0.0$, $t = 0.09$, $t = 0.15$, and $t = 0.97$, where $h = 0.0977$, $h = 0.0745$, and $h = 0.0089$, respectively.

8. T. F. Chan, S. H. Kang, and J. Shen. Euler's elastica and curvature-based inpainting. *SIAM Appl. Math.*, 63(2):564–592, 2002.
9. U. Clarenz, U. Diewald, G. Dziuk, M. Rumpf, and R. Rusu. A finite element method for surface restoration with smooth boundary conditions. *Computer Aided Geometric Design*, 21(5):427–445, 2004.
10. K. Deckelnick and G. Dziuk. Error analysis of a finite element method for the Willmore flow of graphs. *Interfaces and Free Boundaries*, 8:21–46, 2006.
11. Klaus Deckelnick and Gerhard Dziuk. Error analysis for the elastic flow of parametrized curves. *Preprint Fakultät für Mathematik und Physik, Universität Freiburg*, 14-07, 2007. to appear in *Math. Comp.*
12. U. Diewald, S. Morigi, and M. Rumpf. A cascadic geometric filtering approach to subdivision. *Computer Aided Geometric Design*, 19:675–694, 2002.
13. M. Droske and M. Rumpf. A level set formulation for Willmore flow. *Interfaces and Free Boundaries*, 6(3):361–378, 2004.
14. G. Dziuk. Finite elements for the Beltrami operator on arbitrary surfaces. In S. Hildebrandt and R. Leis, editors, *Partial Differential Equations and Calculus of Variations*, Lecture Notes in Mathematics 1357, pages 142–155. Springer, 1988.
15. G. Dziuk. An algorithm for evolutionary surfaces. *Numer. Math.*, 58:603–611, 1991.

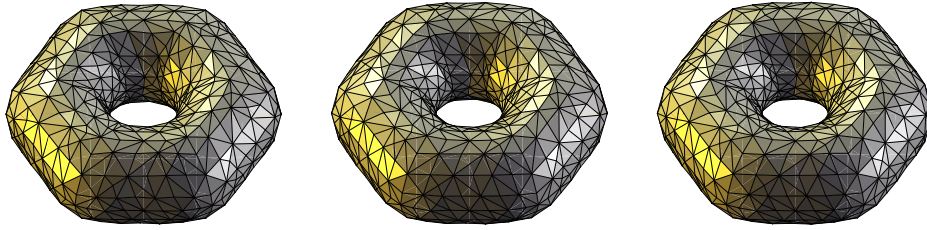


Fig. 8. From the evolution towards the Clifford torus (cf. Figure 7) discrete surfaces at time $t = 0.3735$ are shown based on a computation with time step sizes towards a sphere for an initial macro torus with 1224 elements for different time steps sizes (from left to right) $\tau = h^4$, $\tau = h^2$, and $\tau = h$, where $h = 0.0745$.

16. G. Dziuk, E. Kuwert, and R. Schätzle. Evolution of elastic curves in \mathbb{R}^n : existence and computation. *SIAM J. Math. Anal.*, 33, no. 5(5):1228–1245 (electronic), 2002.
17. Gerhard Dziuk. Computational parametric Willmore flow. *Preprint Fakultät für Mathematik und Physik, Universität Freiburg*, 13-07, 2007.
18. E. Kuwert and R. Schätzle. The Willmore flow with small initial energy. *J. Differential Geom.*, 57(3):409–441, 2001.
19. E. Kuwert and R. Schätzle. Gradient flow for the Willmore functional. *Comm. Anal. Geom.*, 10(5):1228–1245 (electronic), 2002.
20. E. Kuwert and R. Schätzle. Removability of Point Singularities of Willmore Surfaces. Preprint SFB 611, Bonn, 2002.
21. S. Luckhaus and Th. Sturzenhecker. Implicit time discretization for the mean curvature flow equation. *Calc. Var.*, 3:253–271, 1995.
22. D. Mumford. Elastica and computer vision. In C. Bajaj, editor, *Algebraic Geometry and Its Applications*, pages 491–506. Springer, New York, 1994.
23. M Nitzberg, D. Mumford, and T. Shiota. *Filtering, Segmentation and Depth (Lecture Notes in Computer Science Vol. 662)*. Springer-Verlag Berlin Heidelberg, 1993.
24. A. Polden. Closed Curves of Least Total Curvature. *SFB 382 Tübingen, Preprint*, 13:, 1995.
25. A. Polden. Curves and Surfaces of Least Total Curvature and Fourth-Order Flows. *Dissertation, Universität Tübingen*, page , 1996.
26. S. D. Rane, J. Remus, and G. Sapiro. Wavelet-domain reconstruction of lost blocks in wireless image transmission and packet-switched networks. In *Image Processing. 2002. Proceedings. 2002 International Conference on 22-25 Sept. 2002, Vol.1*, 2002.
27. G. Simonett. The Willmore Flow near spheres. *Diff. and Integral Eq.*, 14(8):1005–1014, 2001.
28. Vidar Thomée. *Galerkin finite element methods for parabolic problems*, volume 25 of *Springer Series in Computational Mathematics*. Springer-Verlag, Berlin, 2nd edition, 2006.
29. T.J. Willmore. *Riemannian Geometry*. Clarendon Press, Oxford, 1993.
30. Shin Yoshizawa and Alexander G. Belyaev. Fair triangle mesh generation with discrete elastica. In *Proceedings of the Geometric Modeling and Processing; Theory and Applications (GMP'02)*, pages 119–123, Washington, DC, USA, 2002. IEEE Computer Society.